ka, Moscow, 1967), pp. 227-229; paragenetic data from Kamenev (2), p. 580. These authors report a ^{206}Pb-^{207}Pb age of 2.12 B.Y.
14. Uranium-lead-thorium isotopic data are presented by N. Saito and K. Sato [in *Antarctic Geology*, R. J. Adie, Ed. (North-Holland, Amsterdam, 1964), pp. 590-596], and field relations are by T. Tatsumi, T. Kikuchi, and K. Kizaki (in *ibid.*, pp. 293-303).
15. In principle, it is possible to obtain a minimum value for the primary age of the rocks from the intersection of the growth curve with the line drawn through 2.5-B.Y. lead and the least radiogenic rock lead. If this rock had lost all of its uranium, the true age would be given. When treated in this manner, the data of Sobotovich *et al.* (7) yield a minimum age of 3.5 B.Y. for the parental premetamorphic rocks.
16. C. M. Gray and V. M. Oversby, *Geochim. Cosmochim. Acta* **36**, 939 (1972).
17. S. B. Jacobsen and G. J. Wasserburg, *Earth Planet. Sci. Lett.* **41**, 245 (1978).
18. The reconstruction by E. J. Barron, C. G. A. Harrison, and W. W. Hay [*Eos* **59**, 436 (1978)] is based on matching the 2000-m bathymetric contour and corresponds closely to Fig. 1.
19. A. R. Crawford and R. L. Oliver, *Geol. Soc. Aust. Spec. Publ.* **2**, 283 (1969).
20. A. Holmes, *Proc. Geol. Assoc. Can.* **7** (No. 2), 99 (1955).
21. Rubidium-strontium isochron age of 2301 ± 18 million years is from O. C. Wickremasinghe [*Proc. 26th Annu. Sess. Ceylon Assoc. Adv. Sci.* (1979), part 1, p. 68], which is cited by A. R. Berger [*Geol. Rundsch.* **62**, 345 (1973)].
22. A. Vinogradov, A. Tugarinov, C. Zhykov, N. Stapnikova, E. Bibikova, K. Knorre, *Rep. 22nd Sess. India Int. Geol. Cong.* (1964), part 10, p. 556 (1964); A. R. Crawford, *J. Geol. Soc. India* **10**, 117 (1969); S. M. Naqvi, V. Divakara Rao, H. Narain, *Precambrian Res.* **6**, 323 (1978).
23. This research was supported by NSF grant DPP 76-80957 to the University of California, Los Angeles. Logistic support for E.S.G.'s fieldwork in 1977-1978 was provided by the Antarctic Division of the Australian Department of Science (Australian National Antarctic Research Expeditions). We thank R. J. Tingey, J. W. Sheraton, and L. A. Offe of the Australian Bureau of Mineral Resources and I. F. Allison of the Antarctic Division for their general assistance in E.S.G.'s fieldwork. We also thank P. C. Grew, W. G. Ernst, and M. Halpern for their critical review of the manuscript.

26 March 1979; revised 9 July 1979

Magnitude of Shear Stress on the San Andreas Fault: Implications of a Stress Measurement Profile at Shallow Depth

Abstract. *A profile of measurements of shear stress perpendicular to the San Andreas fault near Palmdale, California, shows a marked increase in stress with distance from the fault. The pattern suggests that shear stress on the fault increases slowly with depth and reaches a value on the order of the average stress released during earthquakes. This result has important implications for both long- and short-term prediction of large earthquakes.*

The magnitude of the shear stresses acting on the San Andreas fault is a subject of considerable controversy. The conspicuous absence of a localized heat flow anomaly near the fault implies that the average shear stress is less than several hundred bars (*1*, *2*). Although this is relatively consistent with estimates of stress reductions of 1 to 100 bars during earthquakes, laboratory experiments with accepted earthquake analogs (such as stick-slip frictional sliding) suggest that the shear stress level is several kilobars (*3*). Resolution of this uncertainty is essential for understanding the mechanics of the fault system and the nature of large earthquakes such as the 1857 and 1906 events.

Because direct measurement of stress at midcrustal depths is not economically feasible, we estimated the magnitude of shear stress on the fault at those depths by measuring the variation of shear stress with distance from the fault at comparatively shallow depths. In an attempt to penetrate rocks near the surface, where joints and weathering may have led to stress relief, the stress measurements were made in wells by using the hydraulic fracturing technique (*4*), in which a section of a vertical well is hydraulically isolated and the fluid pressure increased until a tensile fracture is produced. A vertical fracture should form parallel to the direction of maximum horizontal compression. The least and greatest principal horizontal compressive stresses are determined from the manner of fracture initiation and extension (*5*); the direction of maximum compression is determined from the fracture azimuth. It is presumed that one of the principal stresses is vertical and caused only by the weight of overlying material (*6*). An ultrasonic borehole televiewer (*7*) is used to determine fracture azimuth. A televiewer survey prior to hydraulic fracturing enables one to determine the distribution of natural fractures in the well and allows selection of initially unfractured intervals for the hydraulic fracturing tests.

To make the stress measurements, four wells, each about 250 m deep, were drilled in the western Mojave Desert near Palmdale, California (Fig. 1). Three of the wells were north of the San Andreas fault and were drilled into Cretaceous quartz monzonite; the fourth was south of the fault and was drilled into a Tertiary sandstone.

Numerous fractures and joints were encountered in the wells, and stress measurements could be attempted only at about six intervals in each well (a 4-m interval of unfractured rock is required for each measurement). The results of successful measurements are presented in Fig. 2. As a measure of the reliability of these determinations, note that when two measurements are made at similar depths, the same results are obtained. Also, the magnitude of both horizontal compressive stresses exceeds the lithostat (*8*).

The manner in which stress varies

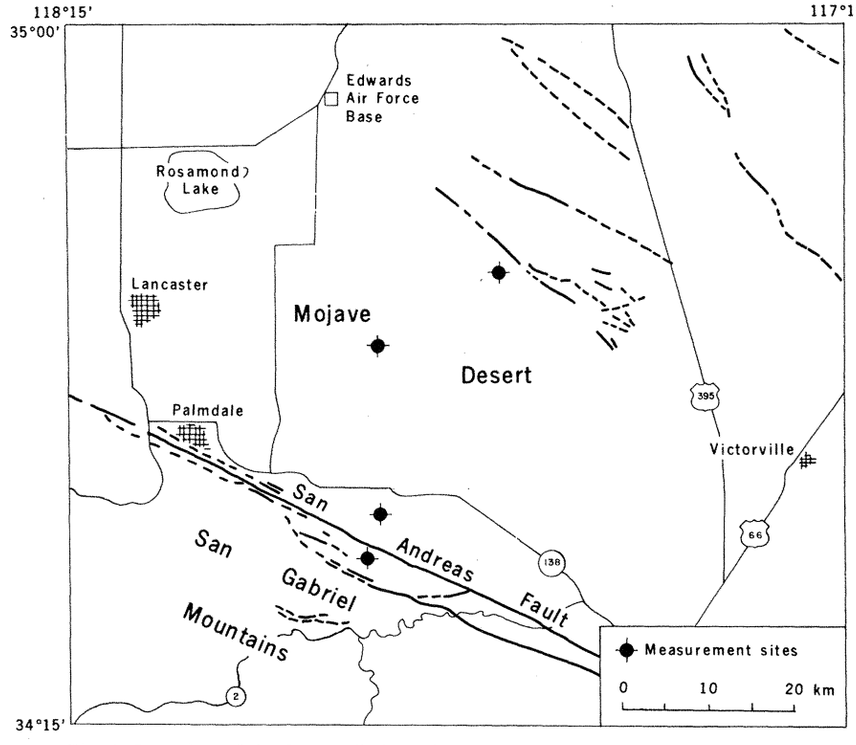

Fig. 1. Location of the four wells in which the stress measurements were made.

0036-8075/79/1026-0445$00.50/0

with depth and distance from the fault has several interesting characteristics. Both horizontal compressive stresses increase with depth in each well and with distance from the fault. The difference in these stresses increases with distance from the fault and increases markedly with depth in the wells distant from the fault.

The most reliable estimates of the direction of maximum horizontal compressive stress (N10°W ± 10°) were obtained from the deepest hydraulic fractures in the two wells closest to the fault. Reliable fracture operations could not be determined in the wells farther from the fault (*9*). Since N10°W (± 10°) is approximately 45° from the strike of the San Andreas fault in this locale, the shearing stress on the fault is simply about one-half the difference between the horizontal principal stresses.

Unfortunately, all of the data in Fig. 2 cannot be considered measurements of the tectonic stress field. Because highly fractured rocks near the surface have almost no frictional strength, there is a stress-relief zone near the surface in which the principal and shear stresses rapidly approach zero. The stress gradients measured in the four wells reflect this phenomenon and, as expected, the degree of natural fracturing in the wells correlates very well with the stress gradients. For example, little or no shear stress gradient was measured in the wells that were closest to the fault, and they were only moderately fractured. The two wells farther from the fault, however, had high shear stress gradients and were markedly more fractured. It would seem, therefore, that a necessary condition for measured stresses to be considered tectonic is that the measurements be made below the stress-relief zone. Since the occurrence of natural fractures was much less below 150 m, only the deepest measurements made in the wells are considered to reflect tectonic stress; the true gradients of stress with depth are unknown. These arguments are further supported by the inconsistent orientation of the stress field near the surface. As mentioned above, the deep measurements in the wells close to the fault gave a geologically reasonable compressive stress direction of N10°W (± 10°). Shallow measurements in the wells, however, gave markedly different directions that were somewhat consistent with surface measurements (*10*).

Figure 3A presents the maximum horizontal shear stress (half the difference in the measured horizontal stresses) computed from the deepest measurements in each well. All the measurements were made at depths of about 200 m (that is, below the zone of intense natural fracturing). Shear stress is seen to increase from a value of 17 ± 4 bars at the wells 2 km from the fault to 54 ± 4 bars at the wells more than 20 km from the fault. Also shown in Fig. 3A are fits to the data from simple model calculations. The modeling evaluates the horizontal shear stress in an elastic plate caused by resistive traction on a vertical, strike-slip fault (Fig. 3B). The influence of forces such as a local basal shear (that conceivably could either drive plate motion or resist it) is neglected, and the net effects and forces arising from "ridge-push" or "trench-pull" are not incorporated into the modeling directly but are simulated by the boundary traction. A two-dimensional finite-element program was used for the computations (*11*). The plate thickness and width are nominally taken to be 24 and 44 km, respectively. Changing the dimensions of the body did not alter the significant aspects of the results. Shear traction on the fault surface was assumed in one case to vary linearly with depth (model 1), and in another case to vary linearly to a depth of 15 km and then remain constant (model 2). The shear stress values shown in Fig. 3B fit the data best and correspond to the curves shown in Fig. 3A. It is not possible to distinguish between the models on the basis of the fit to the data. However, with either model, shear stress on the fault reaches only about 100 bars at a depth of 15 to 20 km.

Although the models are not unique, the increase in shear stress on the fault at shallow depth must be small in order to fit the data from the two close wells, and St. Venant's principle requires that the mean stress on the fault be about 55 bars to fit the data from the distant wells. The data and analysis are, however, insensitive to superposition of a shear stress that varies with depth on the fault but whose average value is close to zero. This, for example, would allow a small frictional stress at zero depth to be incorporated into the model to represent cohesion.

Other models of the San Andreas "earthquake machine" have been proposed and can be tested against our data.

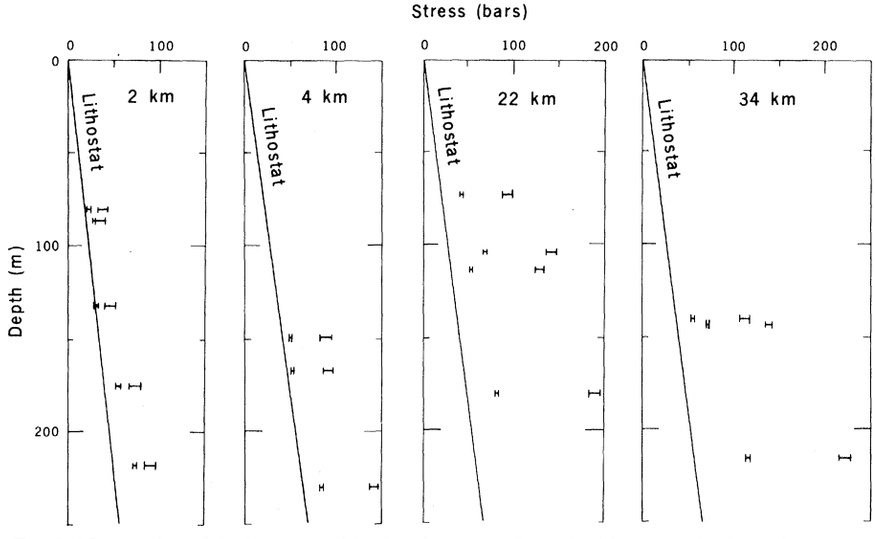

Fig. 2. Magnitudes of the least (small bar) and greatest (large bar) horizontal principal stresses, determined by hydraulic fracturing. Lithostat for each well is the presumed vertical stress based on the appropriate rock density.

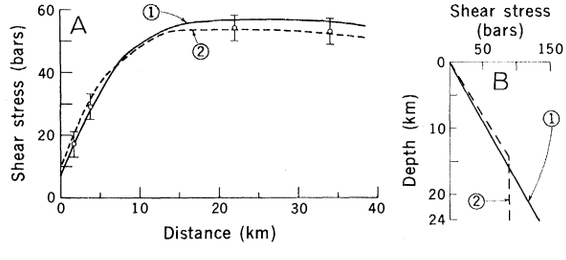

Fig. 3. (A) Shear stress (one-half the difference in the horizontal stresses) as a function of distance from the San Andreas fault, determined from the deepest measurement in each well. Curves are based on the theoretical model shown in (B). (B) Model of traction at the fault trace as a function of depth. Stress is assumed to increase with depth; the magnitude scale was controlled by fitting data shown in (A).

Of particular interest is the basal drag (or brittle) thermomechanical model proposed by Lachenbruch and Sass (*2*) that explains the regional heat flow data. This model is similar to that shown in Fig. 3; shear stress increases rapidly with distance from a weak fault, and a resistive shearing traction at the base of the plate balances the change in horizontal shear. The increase in shear stress with distance from the fault is consistent with the Lachenbruch and Sass model, too. However, prior to rigorous pursuit of any model, reliable vertical stress gradients should be determined.

If shear stress on the San Andreas fault is limited to about 100 bars, the fault is yielding at an extremely low stress. Furthermore, nearly total stress release occurs during earthquakes. It is not clear how this release occurs. The applicability of laboratory-derived frictional coefficients to faulting has been demonstrated for induced earthquakes at the Rangely oil field in Colorado, active normal faults in the Texas coastal area, and elsewhere (*12*). Furthermore, geodetic data appear to verify the basic concept of elastic strain energy accumulation and release along the San Andreas fault. Thus, sliding experiments do seem to be a reasonable analog for earthquakes. However, since the frictional coefficients of all common rock types and minerals are similar, explanations of low fault strength cannot be based on fault zone composition (*13*). One means for lowering the strength of a fault is by reducing the effective stress normal to the fault plane with high (nearly lithostatic) pore pressure. Although anomalously high pore pressure has been proposed to exist throughout the region of the San Andreas fault (*14*), the maintenance of high pore pressure throughout the active history of the fault would require either extremely low regional permeability or some mechanism for regenerating pore pressure within the fault zone itself.

In terms of earthquake prediction, it is clear from these results that if the fault zone is anomalously weak and stress is almost totally relieved during great earthquakes, the accuracy of long-term prediction could be greatly enhanced by stress measurements in critical areas. Furthermore, fault zone monitoring for short-term prediction may be quite straightforward if generation of pore pressure within the fault zone is the mechanism responsible for weakening the fault.

MARK D. ZOBACK
JOHN C. ROLLER
U.S. Geological Survey,
Menlo Park, California 94025

References and Notes

1. J. N. Brune, T. L. Henyey, R. F. Roy, *J. Geophys. Res.* **74**, 3821 (1969).
2. A. H. Lachenbruch and J. H. Sass, *Proceedings of the Conference on Tectonic Problems of the San Andreas Fault System* (Stanford Univ. Press, Stanford, Calif., 1973), p. 192.
3. T. C. Hanks [*Pure Appl. Geophys.* **115**, 441 (1977)] reviews stress reduction data, and J. D. Byerlee [*ibid.* **116**, 615 (1978)] reviews data on rock friction.
4. M. K. Hubbert and D. G. Willis, *Trans. Soc. Pet. Eng. AIME* **210**, 153 (1957); R. O. Kehle, *J. Geophys. Res.* **69**, 249 (1964).
5. M. D. Zoback, J. H. Healy, J. C. Roller, *Pure Appl. Geophys.* **115**, 135 (1977).
6. A review of numerous stress measurements [A. McGarr and N. C. Gay, *Annu. Rev. Earth Planet. Sci.* **6**, 405 (1978)] indicates that this assumption is usually valid.
7. J. Zemanek, E. E. Glenn, C. J. Norton, R. L. Caldwell, *Geophysics* **35**, 254 (1970).
8. In a strike-slip faulting regime, the lithostatic stress is assumed to be of intermediate value between the horizontal stresses. Whether this assumption applies when deeper measurements are made near the San Andreas fault has not been determined.
9. The higher the compressive tangential (hoop) stress at the azimuth of the fracture, the harder it is to detect. Thus, fracture orientations from the wells distant from the fault could not be determined as reliably as those from wells near the fault.
10. M. C. Sbar, T. Engelder, R. Plumb, and S. Marshak [*J. Geophys. Res.* **84**, 156 (1979)] report surface stress measurements in this area. The measurements at the well sites near the fault show considerable scatter in the direction of maximum compression.
11. The two-dimensional finite-element program used for the analysis was kindly provided by W. D. Stuart. To simulate the moving plate resisted by shear traction on a vertical edge, the actual boundary conditions consisted of applying a traction to one of the vertical edges and fixing the other.
12. C. B. Raleigh, A. McGarr, M. D. Zoback, *Eos* **58**, 1227 (1977).
13. The clay mineral montmorillonite is apparently unique and has been found to have low strength at high pressure [Byerlee (*3*)]. However, even if the fault zone were composed entirely of montmorillonite, its strength would be reduced by only a factor of about 3.
14. F. A. F. Berry, *Bull. Am. Assoc. Pet. Geol.* **57**, 1219 (1973).

4 February 1979; revised 24 May 1979

Seasonal Oxygen Isotopic Variations in Living Planktonic Foraminifera off Bermuda

Abstract. *Seasonal variations in the oxygen-18/oxygen-16 ratio of calcite shells of living planktonic foraminifera in the Sargasso Sea off Bermuda are a direct function of surface water temperature. Seasonal occurrence as well as depth habitat are determining factors in the oxygen isotopic composition of planktonic foraminifera. These relationships may be used to determine the seasonal temperature contrast of oceans in the past.*

The $^{18}O/^{16}O$ ratio in calcite is dependent on the temperature and isotopic composition of seawater (*1*). During the Pleistocene, changes in global ice volume induced characteristic changes in the ^{18}O content of the oceans. Thus, the oxygen isotopic composition of calcareous foraminifera in deep-sea sediments provides important stratigraphic records of temporal changes in both global ice volume and ocean water temperatures (*2*).

To fully utilize the ^{18}O content of planktonic foraminifera as a paleoecological tool, it is necessary to identify the factors that determine the $^{18}O/^{16}O$ ratio of different species. In isotopic studies of fossil planktonic foraminifera it is generally assumed that calcite secretion takes place in isotopic equilibrium with ambient seawater, although a few studies of living planktonic foraminifera have suggested the contrary (*3*, *4*). An important consideration is that planktonic foraminiferal shells reflect a range of hydrographic conditions depending on their life-spans, depth habitat preferences, and vertical migration. In addition, planktonic foraminifera exhibit a characteristic seasonal succession in species composition in temperate regions (*5*), resulting in a death assemblage in deep-sea sediments composed of species that lived in the same region but during different seasons and therefore under different hydrographic conditions.

To investigate some of these variables, we determined the oxygen isotopic composition of six species of living planktonic foraminifera collected in surface plankton tows at a station 6 km southeast of Bermuda on an approximately biweekly schedule during an 18-month period (July 1975 to December 1976) (*6*). Hydrographic data were collected biweekly at station S (32°06′N, 64°39′W) about 16 km from our plankton station (*7*).

Isotopic determinations were made on monospecific samples of the following species (*8*): *Globigerinoides ruber* (pink and white varieties separately), *Globigerinoides conglobatus*, *Globigerinella aequilateralis*, *Globorotalia truncatulinoides*, *Globorotalia hirsuta*, and *Pulleniatina obliquiloculata*. *Globigerinoides ruber* had the best sample coverage because it occurred throughout the year in the surface waters off Bermuda. The foraminiferal shells were grouped in various size classes to determine possible isotopic differences due to growth rate or ontogenetic stage. No systematic differences between different size fractions of the same species were found (*9*).

Our results show that seasonal varia-

0036-8075/79/1026-0447$00.50/0